Geologia Croatica
Journal of the Croatian Geological Survey and the Croatian Geological Society
2023 | 76/1 | 47–56 | 10 Figs. | www.geologia-croatica.hr

The Žune Ba-F epithermal deposit: Geophysical characterization and exploration perspective

Jasna Orešković[1,*], Aleksej Milošević[2], Saša Kolar[1] and Sibila Borojević Šoštarić[1]

[1] University of Zagreb, Faculty of Mining, Geology and Petroleum Engineering, Pierottijeva 6, HR-10000 Zagreb, Croatia; (*corresponding author: jasna.oreskovic@rgn.unizg.hr)
[2] University of Banja Luka, Faculty of Mining, Bulevar vojvode Petra Bojovića 1A, 78000 Banja Luka, Bosnia and Herzegovina

doi: 10.4154/gc.2023.04

Article history:
Manuscript received December 27, 2021
Revised manuscript accepted January 23, 2023
Available online February 23, 2023

Keywords: Barite-fluorite deposit, electrical resistivity tomography (ERT), inversion, forward modelling

Abstract

The Žune barite-fluorite ore body in northwestern Bosnia and Herzegovina has been explored using geophysical methods to determine the spatial distribution of the mineralization. The mineralization occurs in a 50 m long ESE-WNW fault zone in the form of a subvertical barite-fluorite vein, transforming to strings of tiny barite veins and impregnations at the immediate contact with the host dolostone. The geophysical research included 2D electrical resistivity tomography (ERT) measured along four profiles. In addition to resistivity inversion results, forward modelling has been performed along two profiles transecting the mining cut. Prior to surface geophysical measurements, detailed geological field mapping of the ore body and host rocks was undertaken. The main faults defined by geological field mapping, have been confirmed with geophysical results as well as the contact of the host dolostone with Lower to Middle Triassic sandstones. The contact is defined to the south of the deposit. However, based on the resistivity model, the position of the contact is about ten metres further south. The forward modelling results revealed that the barite-fluorite vein in the area of the mining cut is limited to a depth of about 10 m and the length is about 70 m. The vein is up to 5 m thick and almost 10 m wide. There is no indication for barite-fluorite mineralization in the area south of the studied mining cut with predominant Triassic sandstones, while anomalies that may be associated with ore bodies are present in the northern and northeastern parts, composed of Carboniferous dolostone.

1. INTRODUCTION

The Žune ore deposit in Bosnia and Herzegovina is part of the Ljubija ore field and is located about 2.5 km west of the town of Ljubija (Fig. 1). The Ljubija ore field is situated within the Upper Palaeozoic sequence of the Sana-Una Palaeozoic complex of the Inner Dinarides. In the wider area of Ljubija, there are smaller and larger bodies of mineralization (metres to hundreds of metres in size), mainly involving Fe carbonates with subordinate Fe, Pb, Zn and Cu sulphides that usually occur in a later phase, as well as slightly younger barite and fluorite mineralization (PALINKAŠ et al., 2016). Of the numerous occurrences of barite in the region, the most interesting (from an economic perspective), is the phenomenon with fluorite in the Donja Ljubija zone, on the Dolinac-Žune-Dobrića Do line (ČIČIĆ, 1976). The Žune barite-fluorite deposit is a vein-type deposit situated in the Upper Palaeozoic dolostone and close to the contact with Lower Triassic schists and sandstones. In the Žune area, barite was exploited by the surface mining method until 1961. Total reserves were 10.000 t, containing 82-98 % of barite, 0.3-1.3 % of SiO_2, 0.4-1.5 % of Al_2O_3, 0.1-0.4 % of Fe_2O_3 and 0.01-6.02 % of CaO. Exploitation ceased when the barite to fluorite ratio became so unfavourable that the economic separation of barite and fluorite could no longer be carried out with the available technology (JEREMIĆ, 1958).

The aim of this study is to explore the Žune ore deposit in more detail and to define the depth of the ore body and spatial distribution of the mineralization. Therefore, detailed geological mapping of the Žune mining cut and surrounding area was carried out indicating that the ore body is laid out vertically with an east-west extension, while a transverse fault with an approximate north-south direction divides the body into the eastern and western parts (Fig. 2). The possibility of a coherent deposit with several ore bodies, apart from the carboniferous dolomites as host rocks, is indicated by the regional fault of the east-west direction. Several long faults of mostly Dinaric extension intersect the deposits and separate them to about ten blocks.

Exploration of the Žune barite-fluorite mineral deposit is challenging due to the complex structural setting driven by subvertical faults and a number of joint-systems (BOROJEVIĆ ŠOŠTARIĆ et al., 2022). Therefore, geophysical methods can help identify areas of a blind ore mineralization since mineral deposits usually have physical properties that contrast with their host rocks (e.g. BISHOP & EMERSON, 1999; MEJU, 2002). Depending on the physical properties of rocks associated with the mineral deposit and in contrast with surrounding material, different geophysical methods can be applied (FORD et al., 2007). Electrical resistivity is a physical property of rocks that generally shows a contrast between mineralized units and surrounding rocks (EVRARD et al., 2018). The current study focuses on the evaluation of a barite-fluorite deposit where barite veins and the barite-fluorite ore are hosted in layered and brecciated dolostone. The barite-fluorite deposits resistivities are expected to be high (e.g. AKPAN et al., 2014; BATISTA-RODRÍGUEZ & PÉREZ-FLORES, 2021) compared to the surrounding rocks. This makes barite veins detectable by electrical and electromagnetic methods. The density of barite is also high, therefore the gravity method can be applied utilizing the high density contrast that exists between barite, especially massive ore bodies, and most of the host rocks (BARNES et al., 1982). In the present case, the gravity method was not applied due to the small size of the ore bodies and very steep flanks of the mining cut. Therefore, electrical resistivity tomography (ERT) has been applied to characterize the ore deposit. Two-dimensional

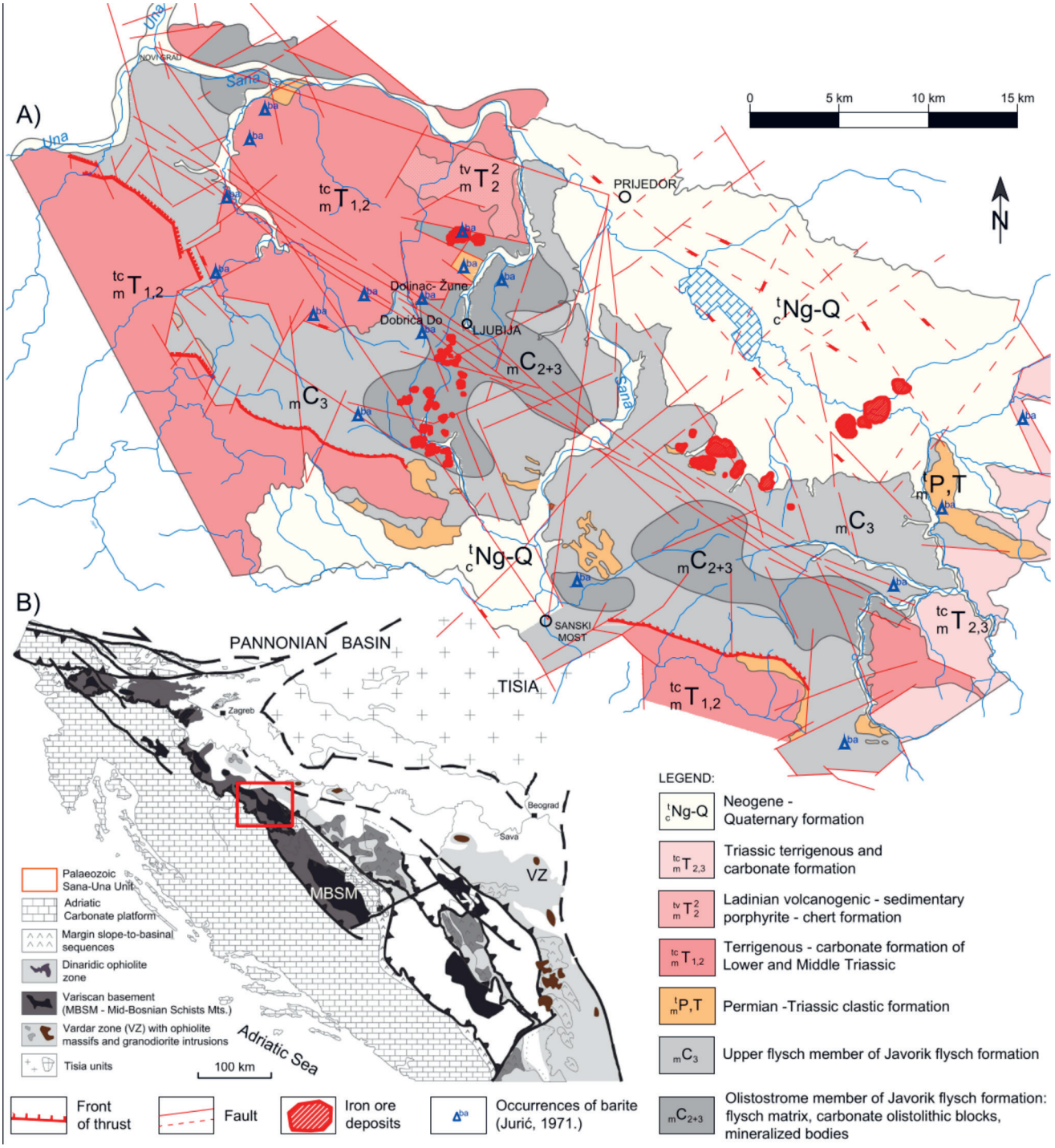

Figure 1. (A) Geological map of the Sana-Una complex showing locations of the iron ore deposits and barite occurrences (modified after GRUBIĆ et al., 2015) and (B) geological map of the main tectonic units in the Northwestern and Central Dinarides with the location of the Žune ore body (modified after PAMIĆ (1993), PAMIĆ et al. (1998), SCHMID et al. (1998), WILLINGSHOFER (2000) and TOMLJENOVIĆ (2002)).

models of the resistivity distribution in the study area are obtained and correlated to geological mapping data. Finally, the results on the dimensions and characterization of the Žune deposit and the possible presence of barite deposits north and south of the Žune mining cut are discussed.

2. GEOLOGICAL SETTING

2.1. Regional setting

The Dinaric Palaeozoic basement units with corresponding Triassic cover are overthrust onto the Adriatic carbonate platform in a distinct NW-SE trending zone extending for almost 700 km and separating the External from the Internal Dinarides units (PAMIĆ et al., 1998; Fig. 1A, B). At the north-westernmost and central part of the Dinaride basement outcrops in a zone <100 km in cross-section, widening toward the southeast to almost 400 km in cross section. The Palaeozoic units vary in age from the Ordovician (Mid-Bosnian Schists Mts.; HRVATOVIĆ, 2006) to the late Permian and Permo-Triassic, as well as the degree of metamorphism that generally increases from the northwesternmost, non-metamorphosed part, toward the central part of the Dinarides showing greenschist to lower amphibolite facies metamorphism (BOROJEVIĆ ŠOŠTARIĆ et al., 2009 and references therein).

The Sana-Una Palaeozoic complex is located to the east of the Una River in the north-western part of Bosnia and Herzegovina. To the northwest, the Sana-Una Palaeozoic complex is separated from its continuation, the Trgovska gora Palaeozoic region in Croatia by the Una River and surrounded by the Lower to Middle Triassic terrigenous-carbonate strata.

2.2. Local geological setting

A wider area of the Žune deposit displays two main lithostratigraphic units (Fig. 2):

(1) The Carboniferous flysch with olistostromes (the Olistostrome member of GRUBIĆ et al., 2015) is a deep-sea unit of variable thickness (between 100 to 300 m), composed of flysch matrix embedding carbonate olistolith segments and blocks of decametres to a hundredmetres in size. Fossiliferous olistoliths are of Devonian, Early and Later Carboniferous ages (JURIĆ, 1971), setting the age of the unit as Middle to Upper Carboniferous (GRUBIĆ & CVIJIĆ, 2003). This agrees with recent palaeontological data according to which the carbonate blocks are of Bashkirian age (MILOŠEVIĆ et al., 2021). Carbonate olistoliths are composed of black micrites, dark grey organogenic and fossiliferous sparites, dolomitic limestones and dolostone. They are often metasomatised and mineralized containing siderite, ankerite and iron-rich carbonate (GARAŠIĆ & JURKOVIĆ, 2012; STRMIĆ-PALINKAŠ et al., 2009; PALINKAŠ et al., 2016).

(2) Lower to Middle Triassic terrigenous formations are represented by carbonate clastic development with intercalations of terrigenous, micaceous limestone, siltstone and sandstone, and in the wider area colourful marls, peloid rocks and breccia (GRUBIĆ & PROTIĆ, 2003).

Mineralization

The Žune barite-fluorite ore body is embedded in porous tectonized dolostone of the Carboniferous Olistostrome member and close to the contact with the Lower to Middle Triassic terrigenous carbonates (Fig. 3), in the ESE-WNW trending Variscan fault zone. Thin-bedded host dolostone occupies the central part of the deposit and the lower parts of the mining cut (Figs. 3 and 4). The thickness of the dolostone layers ranges from 2 to 5 cm, sometimes up to 20 cm. The stratification is well-defined and dips to the east-southeast. The host dolostone is subvertical with a steep slope to the north-northeast, thickness varies from 3 to 20 m along exposed length of 50 m. A 36.5-metre-long exploration drift leaves the ore body after 20.5 metres (Fig. 3).

The Variscan fault zone likely functioned as a pathway for the circulation of hydrothermal fluids, acting as the main control factor for barite-fluorite mineralization. The mineralization is vein-type, composed of the main barite-fluorite vein (3 to 9 m thick), emplaced sub vertically with an east-west extension. The barite to fluorite ratio is 80:20. The contact zone between dolostone and mineralization consists of metasomatically recrystallized host dolostone, quartz associated with accessory minerals and pyrite with strings of tiny barite veins and impregnations and is mostly brecciated. Accessory minerals provide evidence for pre-mineralization conditions with temperatures exceeding 300°C (BOROJEVIĆ ŠOŠTARIĆ et al., 2022). The central part of the vein consists of pure barite, some fluorite and accessory sulfide minerals (JEREMIĆ, 1958). Syn-mineralization conditions from NaCl-$CaCl_2$-H_2O fluids under temperature of 100–310 °C were determined by PALINKAŠ et al. (2016). Furthermore, based on the fluorite-hosted fluid inclusions, the authors reported evidence for a low-pressure boiling event under epithermal conditions. Hydrothermal fluids were interpreted as being a mixture of high-temperature-high-salinity Permian evaporitic sea water, diluted by low-temperature-low-salinity marine or meteoric waters.

At the lowest level, the ore body appears to narrow, while it broadens toward the higher levels, retaining similar structural

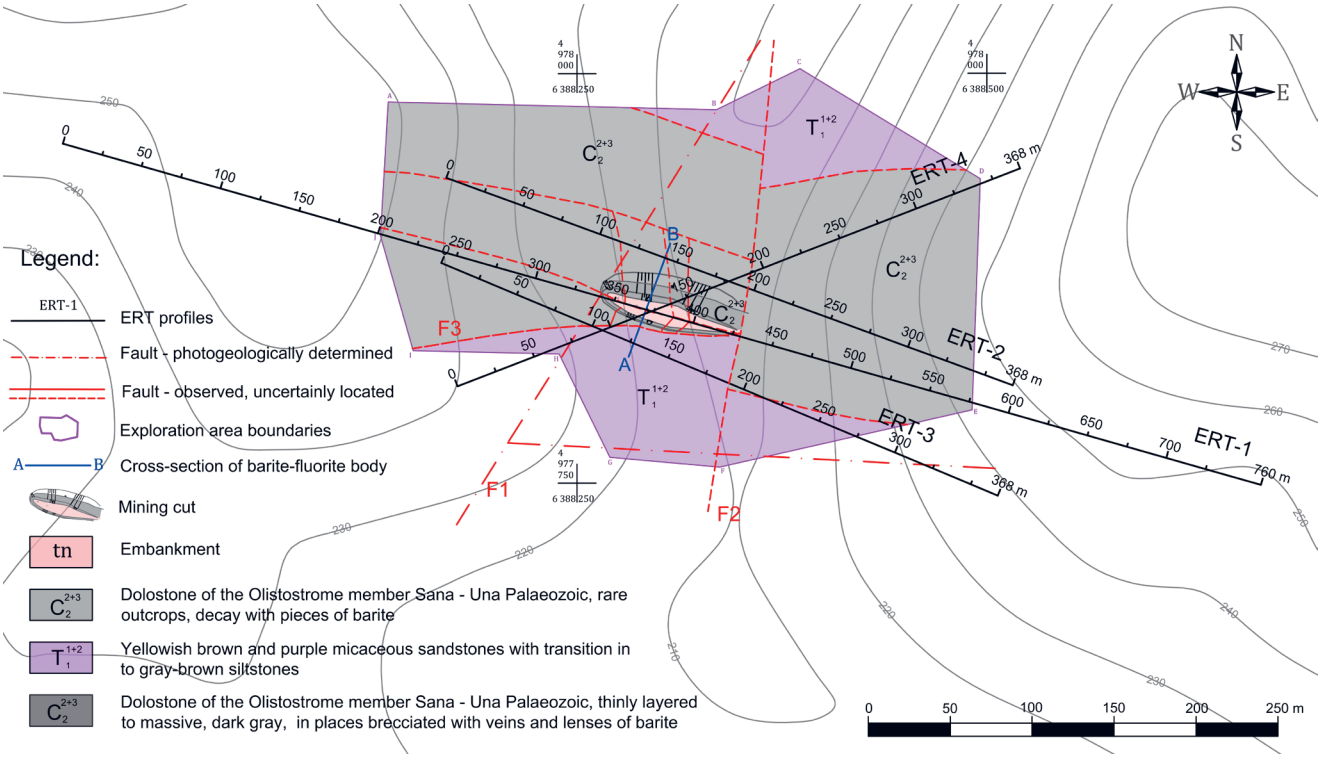

Figure 2. Location map of the Žune survey area with the positions of ERT profiles and the mining cut. The main geological units and faults within exploration area are displayed.

Geologia Croatica

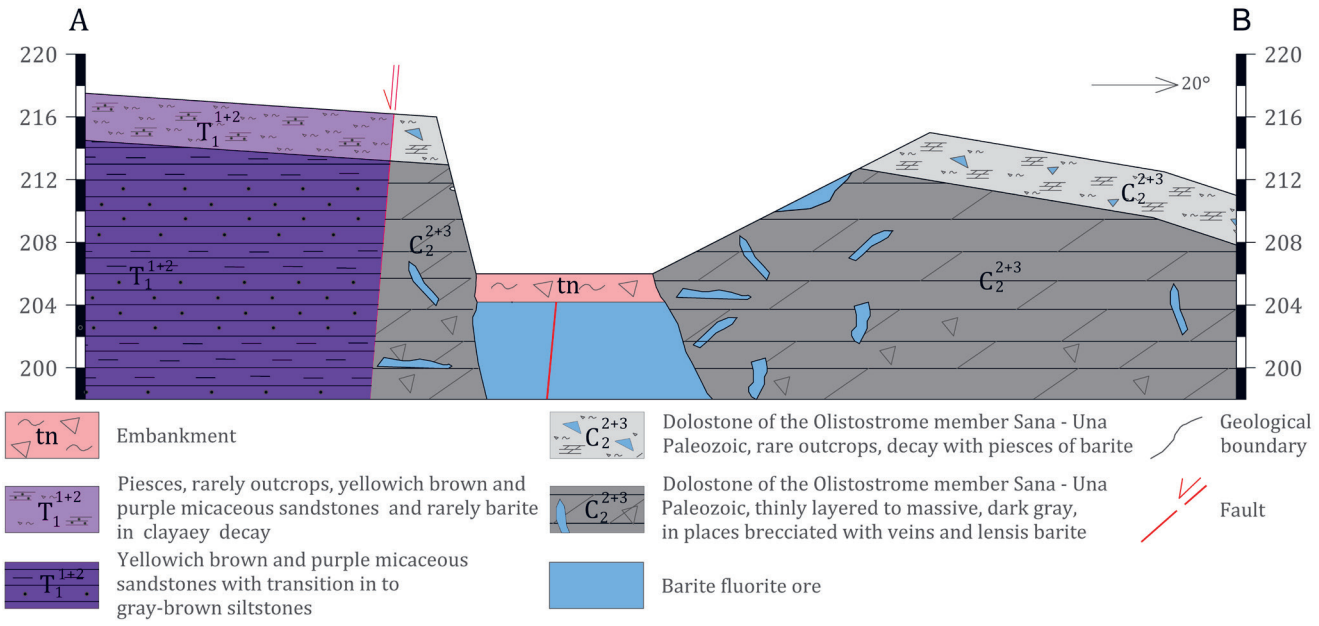

Figure 3. A cross–section of the Žune barite–fluorite body along the line AB in a SSW-NNE direction. Location of the cross-section is marked on the map in Fig. 2 (modified after JEREMIĆ, 1958).

features (JURIĆ, 1971). The upper part of the ore body is enriched with limonite of supergene origin, related to oxidation of minor sulfide mineralization associated with the barite-fluorite (JEREMIĆ, 1958).

Dolostone from both sides of the main barite-fluorite vein contains irregular barite veinlets imprinted in various fracture directions (stockwork to impregnation type), usually across the bedding or isolated barite lenses (Figs. 3 and 4). Barite lenses are 20 x 30 cm in size and can sometimes be traced for as far as 10 m. The contact with the surrounding dolostone is usually sharp.

In the southern part of the deposit, Lower to Middle Triassic formations are exposed and consist mainly of intercalations of reddish and purple quartz sandstones with sericite and shaly clays. The contact with the dolostone is tectonic.

The central part of the exploration drift is covered with a 2 m thick barite embankment consisting of variable-size dolomite, barite and barite with fluorite blocks in clayey-sandy detritus, representing a remnant of previous mining activities (Fig. 3).

3. METHODOLOGY

3.1. Geophysical data acquisition

Geophysical data acquisition was carried out covering the wider area of the abandoned mining cut in Žune (Fig. 2). Electrical resistivity tomography (ERT), a surface geophysical method was used to map the prospective baritefluorite area. The ERT technique is used to image both vertical and lateral variations of resistivity along the measured line. As a result, a pseudosection of apparent resistivities is plotted. Four profiles were set up at the Žune survey area and the data were collected using an ABEM SAS 1000 resistivity meter and the ES 10-64 selector. The first ERT line was a 760 m long profile (ERT-1 in Fig. 2) that covered

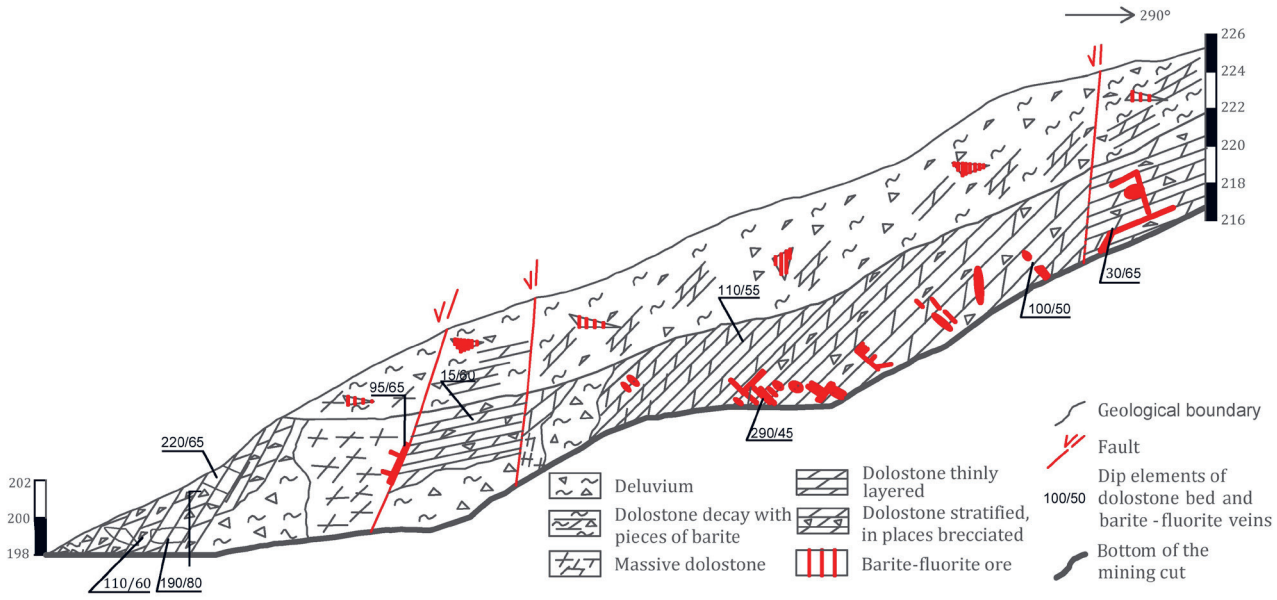

Figure 4. A cross – section of the Žune ore body along the southern side of the mining cut.

the barite-fluorite outcrop in the direction of its longer axes. To cover a larger prospective area, two additional 400 m long ERT lines almost parallel to ERT-1 (ERT-2 and ERT-3 in Fig. 2), and one diagonal line were set up (ERT-4 in Fig. 2). The Wenner electrode configuration with a unit electrode spacing of 10 m was used for the electrical resistivity measurements along lines ERT-1, ERT-3 and ERT-4, while an electrode spacing of 5 m was used along the line ERT-2. Thus, the investigation depth along the longest ERT-1 line is about 135 m and other profiles reach about 70 m at the deepest part. The measured 2D apparent resistivity sections were interpreted using inversion and forward modelling based on the method published by LOKE & BARKER (1996).

3.2. Inversion and forward modelling

The electrical resistivity tomography (ERT) measurements give 2D apparent resistivity pseudosections, and to obtain true resistivity models that reflect the subsurface geology, an inversion of the data is required. The recorded apparent resistivity data along four ERT profiles were interpreted using inversion as well as forward modelling. Automatic inversion of observed data was used to rapidly determine the best resistivity model that fits the measured field data. The boundaries in the inverse model are difficult to define since the transition zone from low to high resistivity is wide, therefore forward modelling was applied in order to interpret the inversion results more reliably. During modelling, the apparent resistivity pseudosection is calculated for an *a priori* defined 2D subsurface model. The advantage of forward modelling is that the model can be lithologically constrained by data from other sources (geological data or results of other geophysical surveys). It also provides the opportunity to test several possible models with different depths of boundaries or lateral extent of structures.

During inversion, an homogenous resistivity 2D model consisting of rectangular blocks was used. The number of blocks and their distribution is set according to the distribution of observed data points in the pseudosection. The inversion is performed using a non-linear smoothness-constrained least-squares optimisation technique (de GROOTHEDLIN & CONSTABLE, 1990; LOKE et al., 2003). The convergence criterion was the relative change in the RMS error between two iterations.

The forward modelling simulation calculates the apparent resistivity pseudosection for a userdefined 2D subsurface model. The results based on this model are inverted and then compared to the results of observed data. This involves dividing the subsurface into a number of blocks using a rectangular mesh, with each block characterized by its resistivity. The size of the blocks, i.e. how finely defined the mesh is, depends on the complexity of the geological structure being modelled. In 2D forward modelling the finitedifference method (DEY & MORRISON, 1979) was used to determine the potential at each node of the mesh.

4. GEOPHYSICAL MODELS

4.1. Inversion of ERT data

The geophysical survey of the Žune barite-fluorite deposit started with the longest profile located through the abandoned mining cut (ERT-1 in Fig. 2) and was followed by three additional profiles of half the length. The measured data along four profiles are interpreted using inversion (Figs. 5-7). During inversion of the measured data, least-square equations are solved using a standard Gauss-Newton method. A relative change in the RMS error of 0.1 was used to test the convergence of calculated apparent resistivity data. The models are displayed with the maximum depth in the central part corresponding to the depth of investigation with the largest electrode spacing (EDWARDS, 1977).

The final inverted resistivity model along ERT-1 was obtained after five iterations with an RMS error of 3.6 % (Fig. 5). The interpreted depth is about 100 m in the central part of the profile. The obtained model provides information about the subsurface in the mining cut and in the surrounding area. The most prominent feature of the resulting model is high resistivity (> 4000 Ωm) in the central part of the profile exactly where the mining cut is located. The high resistivity structure extends to a depth of 5-10 m. At the beginning of the profile, the resistivity is lower (about 200 Ωm), as well as in the second part of the profile at a very shallow depth (to about 10 m). In the deeper parts of the profile the resistivities are rather high (between 1000 and 2000 Ωm), with the greatest values at distances between 250 and 320 m. These resistivities most probably originate from carbonate rocks while lower resistivities in the first 180 m of the profile could be associated with sandstones and the near surface resistivities originate from soil and clay. According to the results of geological mapping presented in Figure 2, the Žune mining cut is bordered by two faults at about 335 m (F1) and 430 m (F2) profile distance. The western fault can be recognized in the inverted model as a sharp resistivity transition near 340 m, while the position of the eastern one is not so clearly visible.

Profiles ERT-2 and ERT-3 are about half the length of profile ERT-1 and are nearly parallel to it (Fig. 6). The ERT-2 is located 40 to 20 m north of the profile ERT-1, and ERT-3 is south of it. Unit electrode spacing on the ERT-2 profile was 5 m, since the electrode spacing is one of the factors affecting the resolution of observed data, besides array configuration and signal-to-noise ratio (CARDARELLI & DE DONNO, 2019). Smaller spacing has been expected to produce better resolution. The inverted model

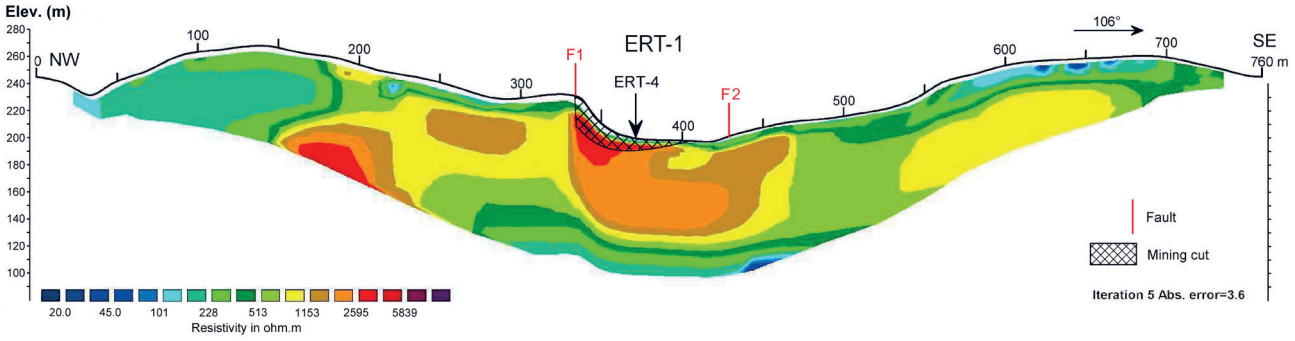

Figure 5. 2D inversion along profile ERT-1 stretching in the direction of the longer axes of the mining cut. The intersection with profile ERT-4 is marked by an arrow, and location of the mining cut is indicated. Positions of the major faults defined within location map in Fig. 2 are indicated with red line at the surface.

Geologia Croatica

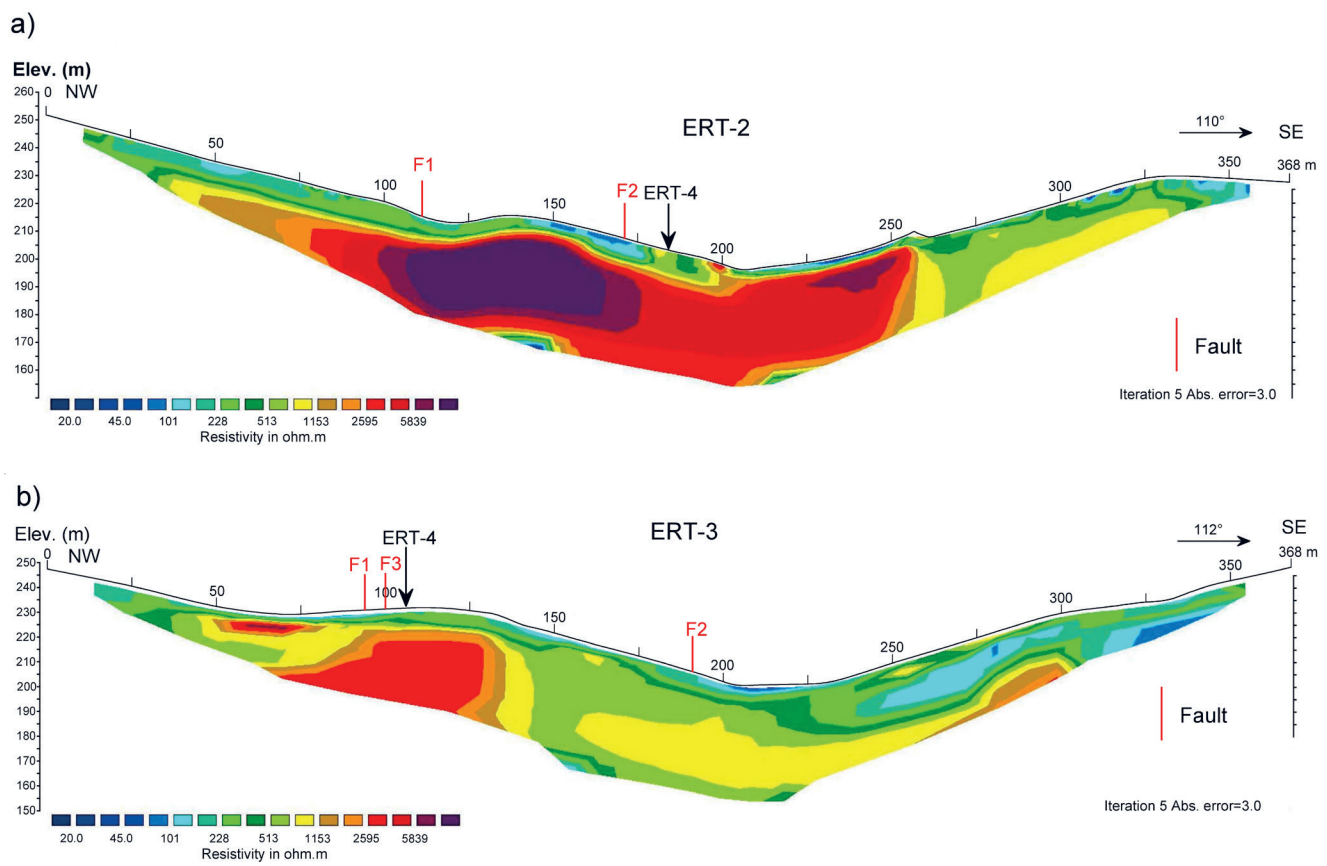

Figure 6. Inverted 2D resistivity models nearly parallel to ERT-1: (a) ERT-2 and (b) ERT-3. The intersection with the profile ERT-4 which is laid diagonally is indicated by an arrow.

of the ERT-2 profile was obtained after five iterations and the RMS error is 3.0% (Fig. 6a). The ERT-2 shows the highest resistivities in the survey area. The high resistivity anomaly stretches approximately from 110 m to 170 m and between 230 and 250 m. The depth of the anomaly can be estimated to be about 5-10 m. A minor high resistivity anomaly is observed at a distance of 200 m close to the surface.

However, the inversion results of profile ERT-3 show that the resistivities south of ERT-1 are generally low, especially near the surface (to 5 m depth) as well as at the western part of the profile at greater depths (Fig. 6b). High resistivity can be observed only at the beginning of the profile, between 50 and 75 m, at shallow depths.

Profile ERT-4 is 370 m long and extends diagonally to the other three profiles in an ESE-WNW direction, and intersects the mining cut transversely at the distance of 110 to 130 m. At the beginning of the profile, the resistivity is about 400 Ωm until the distance of 70 m (Fig. 7). This is significantly lower than the resistivity along the rest of the profile. From a distance of 70 m, the resistivity increases sharply and reaches about 2000 Ωm. This is also expected according to the location map in Figure 2, since the sandstones in the southern part of the Žune deposit are in contact with tectonized dolostone.

The 3D subsurface resistivity image by combining the inverted ERT models of two profiles (ERT-2 and ERT-4) is presented in Fig. 8. The models show that the highest resistivity is found in the central and western part of profile ERT-2, while profile ERT-4 crosses this anomaly at its eastern edge (Figs. 6 and 8). The highest resistivity could be associated with a barite or barite-fluorite deposit, although high resistivity values are also

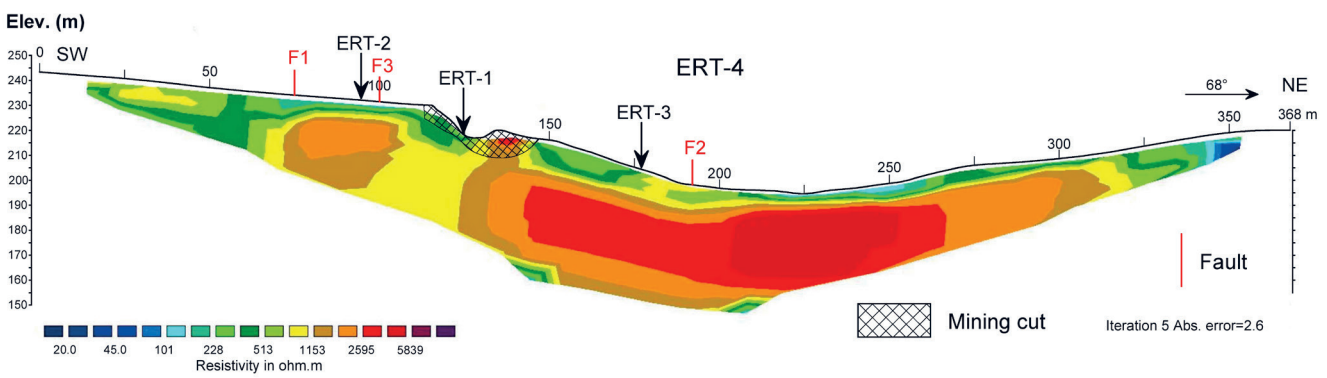

Figure 7. Inverted 2D resistivity model along profile ERT-4 which intersects transversely the mining cut. Intersections with the other three profiles are indicated with arrows.

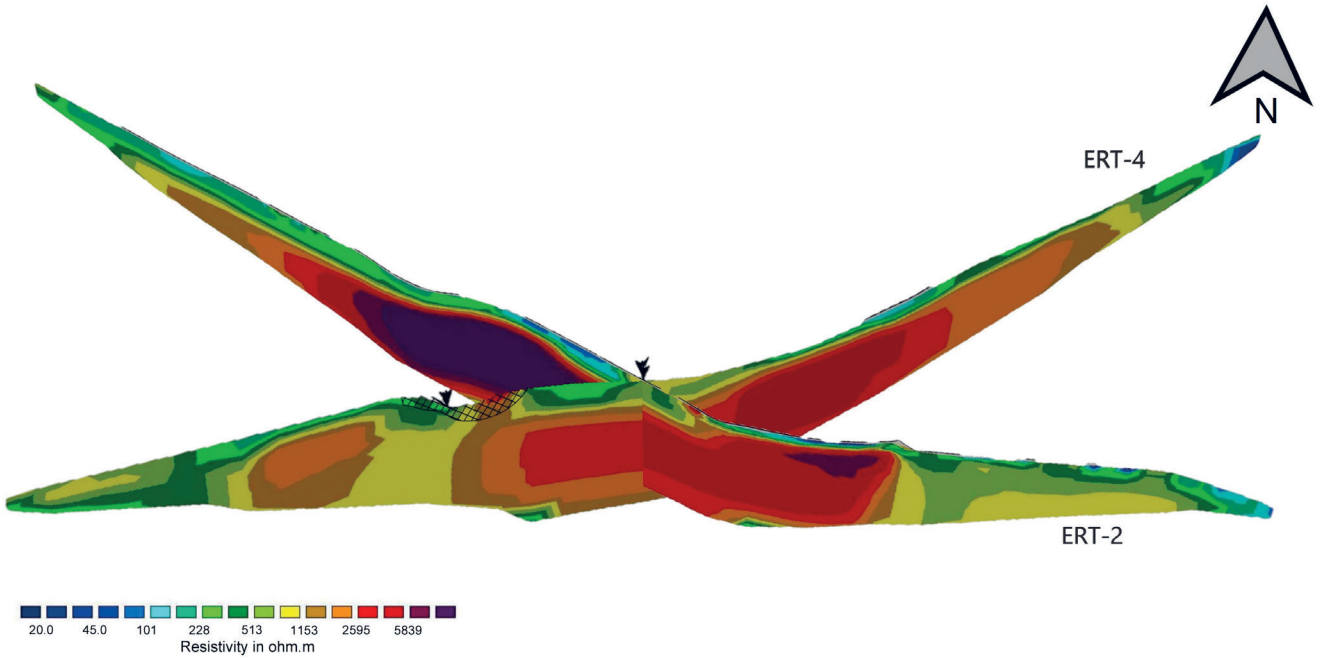

Figure 8. Subsurface resistivity distribution on profiles ERT-2 and ERT-4 displayed in 3D. The hatch pattern marks the position of the mining cut.

expected for dolomites. The eastern part of the exploration area in Figure 2 is poorly explored, but there is evidence for the presence of an ore body based on several excavated barite veins. Profiles ERT-2 and ERT-4 in their easternmost parts include this area, but resistivities are rather low and do not indicate the presence of a major barite or barite-fluorite vein in the eastern part. Also, there are no anomalies south of the mining cut that could be associated with a barite ore body.

4.2. Forward modelling results

In the electrical resistivity tomography method, the problem of ambiguity is present similar to onedimensional resistivity methods, but it has a more complicated 2D character. The ambiguity manifests in the fact that there may be many correct geoelectrical models that fit within the accepted RMS error limits. In addition, ERT survey data are affected by structures located some distance from the survey line. Thus, 2D inverted models include spurious effects due to resistivity changes perpendicular to the surveyed profile (CARDARELLI & DE DONNO, 2019). Only in the case where the geological structure is uncomplicated and can be approximated with a 2D model, can an interpreted resistivity section be related to a structure present directly beneath the survey line (BANIA & ĆWIKLIK, 2013). Furthermore, the inverted model has rather wide transitions between high and low resistivities and the boundary is not easy to define. Therefore, the inverted models and interpretation results were verified by forward modelling along two profiles, ERT1 and ERT4 (Figs. 9 and 10) that provide a more distinctive picture.

In the current study, the geometry of the main structures in the initial models was defined according to the ERT inversion results and, where available, data from detailed geological field mapping. The electrode arrays and unit electrode spacing were the same as in the field layout, but topography was not considered. The response (apparent resistivity), for the defined model is calculated using the finite-difference method, and the results are compared to the ERT inversion results. In addition to the geometry, resistivities in the model need to be defined. Since no laboratory or borehole resistivity measurements were available, the models are based on inversion results and resistivities of the main lithologies published in the literature (SCHÖN, 2011; TELFORD et al., 1990). The resistivities for the same rock type have a wide range of values, sometimes over several orders of magnitude. For example, the resistivity range for sandstones (10 to 10^4 Ωm) and dolomites (10^2 to $7{\cdot}10^4$ Ωm) overlap but sandstones tend to have generally lower resistivity (SCHÖN, 2011; WARD, 1990). However, the resistivity of rocks depends not only on lithology, but also on rock conditions (degree of fracturing) and fluid content. The resistivities of minerals are more specific, and in Ba-F deposits measured resistivity will depend on the barite and fluorite content. Both barite and fluorite as minerals are characterized by high resistivity ($1.2{\cdot}10^7$ Ωm for barite and $7.7{\cdot}10^{13}$ Ωm for fluorite; SCHÖN 2011). In the present study, the Žune barite-fluorite ore body is imprinted in porous dolostone and barite occurs as pure barite accompanied with fluorite in the central part and porous barite in the NE part of the deposit. Fluorite also occurs in lenses or as impregnations within barite veins and dolostone. The deposit is clearly visible on both profiles (ERT-1 and ERT-4) as a shallow high resistivity anomaly and in resistivity models it is defined with $5{\cdot}10^3$ Ωm.

Along profile ERT-1, the main features are a thin body of high resistivity at shallow depths (yellow in Fig. 9) and a high resistivity block to a depth of about 50 m. 2D modelling of the resistivity data confirmed that the anomaly at shallow depth is due to the presence of a 5 m thick block of high resistivity. A greater thickness is unlikely because the inversion results of the block model with a thickness greater than 5 m yield an anomaly that is not consistent with the inversion results of the observed data. The lower resistivity of this block results in a less pronounced anomaly than the measured one (Fig. 9c). The depth to the upper base of the block is about 5 m, since a shallower or deeper structure cannot produce an anomaly that fits the ERT inversion results. According to the location, it belongs to a barite-fluorite deposit within the mining cut. The length of the deposit is about 70 m. This structure is also observed on profile ERT-4, which extends diagonally to ERT-1 (Fig. 10). A small anomaly of high resistivity

Geologia Croatica

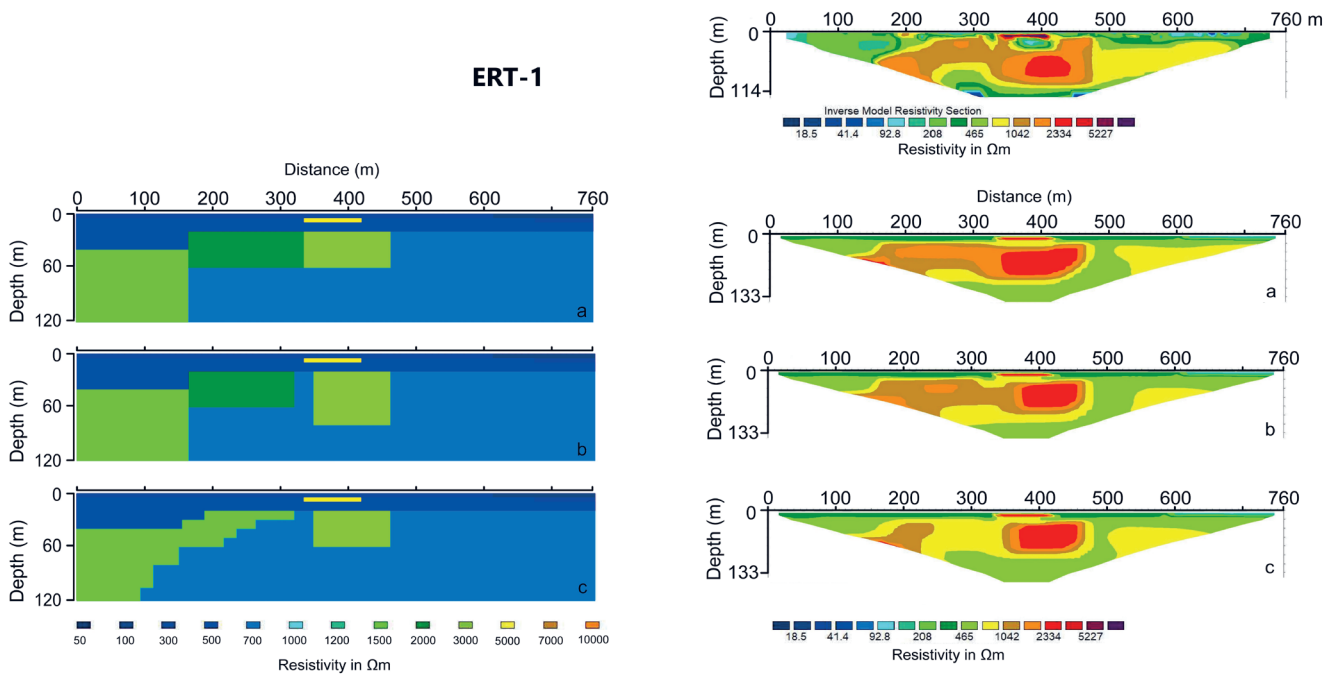

Figure 9. 2D forward modelling along profile ERT-1. The synthetic resistivity models are shown on the left and calculated resistivity pseudosections are on the right. The inverted resistivity model of measured data is at the top.

is interpreted as a block at a distance of 140 to 150 m at a very shallow depth (up to 7 m). The origin of this high resistivity is the same as on ERT-1, but the geophysical signature is slightly different due to the orientation of the profile with respect to the ore deposit.

According to the forward resistivity model of profile ERT-1, the deeper high resistivity anomaly (distance 335 380 m) can be associated with a structure at about 20 m depth (Fig. 9), which is probably massive dolostone. The thickness is between 40 - 60 m.

When a smaller resistivity is defined between two blocks of higher resistivity that can be associated with a fault zone (distance 320 - 350 m in Fig. 9b), very good agreement with the observed data is obtained. A zone wider than 30 m is unlikely. The contact between lower resistivity rocks at the beginning of the profile (probably sandstones) and higher resistivity rocks is defined at a distance of about 160 m (Fig. 9a and b). Forward modelling results indicate that the contact is sharp, as a gradual change between higher and lower resistivities results in a weaker match (Fig. 9c).

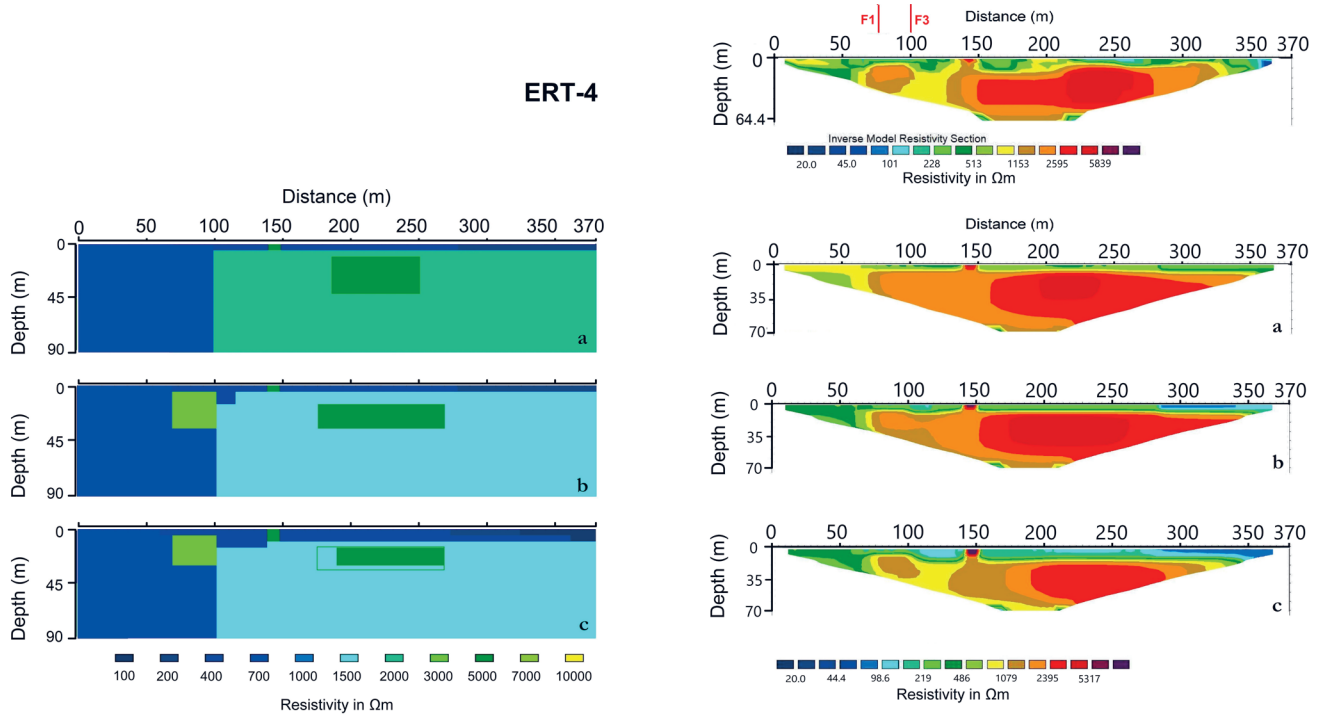

Figure 10. 2D forward modelling along profile ERT-4. Resistivity models are on the left and inversion of calculated resistivity pseudosections on the right. The inverted resistivity model of measured data is at the top.

The initial resistivity model along the profile ERT-4 (Fig. 10a) was constructed according to the inversion results and previous investigations presented in Fig. 2, showing the main geological units and faults within the study area. The contact between the Lower to Middle Triassic sandstones and the dolostone is defined by the F3 fault at the southern part of the deposit (Fig. 2). Profile ERT-4 intersects this contact, and therefore lower resistivities are defined in the first part of the model (left in Fig. 10) to about 100 m. From 100 m to the end of the profile higher resistivities are expected, and a sharp contact between sandstones and dolostone is defined. The main features of the inverted model (Fig. 7 and top of Fig. 10) are a high resistivity anomaly near the surface at a distance of about 140 m, and a deeper anomaly at a distance of 210 to 250 m. Therefore, a shallow, small block of high resistivity was defined at a profile distance of 140-150 m, corresponding to the position of the mining cut and the barite-fluorite deposit. A deeper block of higher resistivity was defined at a distance of 190 to 250 m.

A calculated pseudosection based on the initial model shows a similar resistivity distribution as the observed one in the shallow part, and in the deeper part from a distance of about 150 m (Fig. 10a). However, the anomaly present in the inverted model of observed data between 50 and 100 m is not evident. Therefore, a higher resistivity was introduced down to a depth of 40 m, which required a larger width of the central block (Fig. 10b). Finally, the most probable model (Fig. 10c) is similar to model (b) but includes a greater thickness of a surface low resistivity layer and consequently a greater thickness of the body at the location of the mining cut. A smaller thickness of the central block is possible which extends over a distance of 190 m to 270 m. The contact could be defined at a distance of about 70 m corresponding to F1 in Figure 2, while according to the geological map it is located at a profile distance of 100 m (F3 in Figure 2).

5. CONCLUSIONS

The wider area of the Žune barite-fluorite ore body was investigated using an electrical resistivity tomography method to characterize the ore body and to identify possible new deposits. Four ERT profiles were measured to obtain the resistivity distribution in the subsurface. ERT forward modelling was used to create more accurate resistivity models than those obtained by automatic inversion.

Interpretation of the ERT data confirmed that the mineralization occurs in an ESE-WNW fault zone in the form of a subvertical barite-fluorite vein that is 50 to 70 m long. A strong resistivity anomaly associated with the main barite-fluorite vein is only visible on the longest profile ERT-1, which extends along the direction of the Žune ore body, and on profile ERT-4 which is diagonal to the mining cut. Modelling results indicate that the main barite-fluorite vein is located at a depth of 5 to 10 metres and is approximately 70 m long. The thickness of the vein is up to 5 m. Based on the forward modelling along profile ERT-4, the width of the vein is almost 10 m. According to the location of the most prominent shallow anomaly, the results confirmed the association of the main vein with shallow mineralization.

The main faults, which extend in a northeast-southwest direction, have been confirmed on profiles ERT-1, ERT-2 and ERT-4 but are also recognized on profile ERT-3. The contact of the host dolostone with Lower to Middle Triassic sandstones, defined in the southern part of the deposit (Figs. 2 and 3), has been proved with profile ERT-4. However, based on the resistivity model, the position of the contact is about ten metres further south.

There is no evidence of barite-fluorite mineralization south of the mining cut, in the area with predominant Triassic sandstones. Anomalies that can be associated with ore bodies are present in the northern and northeastern part, composed of Carboniferous dolostone. Profiles ERT-2 and ERT-4 show high resistivity anomalies, and the major one is located to the north of the mining cut. In the eastern part, the anomalies are less pronounced. Their cause could be isolated barite lenses and the presumed occurrences in the form of stockworks and impregnation veins, which show a lower intensity of anomalies than a massive barite-fluorite ore body. Since barite veins are hosted in dolostone that is also characterized by high resistivity values, the existence of a high resistivity anomaly cannot provide complete information about the ore body. Therefore, exploratory drilling is necessary to ascertain results of geophysical exploration.

ACKNOWLEDGEMENT

This work has been financially supported by EIT RawMaterials project no. 17051 Invest RM: Multifactor model for investments in the raw material sector, a part of the Horizon 2020 program. We would like to thank the Invest RM team (https://investrm.eu/) for continuous fieldwork support, helpful advice, and discussion. A special thanks to colleagues from the Mining Institute Prijedor supervised by director Dragoja LAJIĆ for their assistance during the geophysical field survey.

REFERENCES

AKPAN, A.E., EBONG, D.E., EKWOK, S.E. & JOSEPH, S. (2014): Geophysical and Geological Studies of the Spread and Industrial Quality of Okurike Barite Deposit.– Am. J. Environ. Sci., 10/6, 566–574. doi: 10.3844/ajessp.2014.

BANIA, G. & ĆWIKLIK, M. (2013): 2D Electrical Resistivity Tomography interpretation ambiguity – example of field studies supported with analogue and numerical modelling.– Geology Geophysics & Environment, 39/4, 331–339. doi: 10.7494/geol.2013.39.4.331

BARNES, D.F., MAYFIELD, C.F., MORIN, R.L. & BRYNN S. (1982): Gravity measurements useful in the preliminary evaluation of the Nimiuktuk barite deposit, Alaska.– Econ. Geol., 77/1, 185–189. doi: 10.2113/gsecongeo.77.1.185

BATISTA-RODRÍGUEZ, J.A. & PÉREZ-FLORES, M.A. (2021): Contribution of ERT on the Study of Ag-Pb-Zn, Fluorite, and Barite Deposits in Northeast Mexico.– Minerals, 11, 249, 1–16. doi:10.3390/min11030249

BISHOP, J. R. & EMERSON, D. W. (1999): Geophysical properties of zinc-bearing deposits.– Aust. J. Earth Sci., 46/3, 311–328. doi: 10.1046/j.1440-0952.1999.0

BOROJEVIĆ ŠOŠTARIĆ, S., PALINKAŠ, A.L., STRMIĆ PALINKAŠ, S., BERMANEC, V., NEUBAUER, F., SPANGENBERG, J.E. & PROCHASKA, W. (2009): Origin of siderite–barite-polysulfide mineralisation in Petrova and Trgovska Gora Mts., NW Dinarides.– Miner Petrol, 97, 111–128.

BOROJEVIĆ ŠOŠTARIĆ, S., ROGLIĆ, M., MILOŠEVIĆ, A., BRENKO, T. (2022): Žune Ba-F epithermal deposit Part 1: Mineralogical and geochemical characteristics.– Geol. Croat., 75/3, 393–410. doi: 10.4154/gc.2022.24

CARDARELLI, E. & DE DONNO, G. (2019): Advances in electric resistivity tomography: Theory and case studies.– In: PERSICO, R., PIRO, S. & LINFORD, N. (eds.): Innovation in near-surface geophysics, 23–57, Elsevier. doi:10.1016/B978-0-12-812429-1.00002-7

ČIČIĆ, S. **(1976)**: Mineralne sirovine Bosne i Hercegovine: II knjiga – Ležišta nemetala.– Geoinženjering, Sarajevo, 231–446.

DE GROOT-HEDLIN, C. & CONSTABLE, S. (1990): Occam's inversion to generate smooth, two-dimensional models form magnetotelluric data.– Geophysics, 55, 1613–1624. doi: 10.1190/1.1442813

DEY, A. & MORRISON, H.F. (1979): Resistivity modelling for arbitrary shaped two-dimensional structures.– Geophys. Prospect., 27, 1020–1036. doi: 10.1111/j.1365-2478.1979.tb00961.x

EDWARDS, L.S. (1977): A modified pseudosection for resistivity and induced polarization.– Geophysics, 42, 1020–1036.

EVRARD, M., DUMONT, G., HERMANS, T., CHOUTEAU, M., FRANCIS, O., PIRARD, E. & NGUYEN, F. (2018): Geophysical Investigation of the Pb–Zn Deposit of Lontzen–Poppelsberg, Belgium.– Minerals, 8/6, 233. doi:10.3390/min8060233

FORD, K., KEATING, P. & THOMAS, M.D. (2007): Overview of geophysical signatures associated with Canadian ore deposits.– In: GOODFELLOW, W.D. (ed.): Mineral Deposits of Canada: A Synthesis of Major Deposit Types, District Metal-

logeny, the Evolution of Geological Provinces, and Exploration Methods. Geological Association of Canada, Mineral Deposits Division, St. John's, 939–970.

GARAŠIĆ, V. & JURKOVIĆ, I. (2012): Geochemical characteristics of different iron ore types from the Southern Tomašica deposit, Ljubija, NW Bosnia. – Geol. Croat. 65/2, 255–270. doi:10.4154/GC.2012.16

GRUBIĆ, A. & CVIJIĆ, R. (2003): New contribution in geology and metallogeny of the Ljubija iron mine. Institute of Mining Prijedor, Prijedor, 137 p.

GRUBIĆ, A., CVIJIĆ, R., MILOŠEVIĆ, A. & ČELEBIĆ, M. (2015): Importance of olistostrome member for metallogeny of Ljubija iron ore deposits.– Arch. Techn. Sci., 13/1, 1–8. doi: 10.7251/afts.2015.0713.001G

GRUBIĆ, A. & PROTIĆ, LJ. (2003): Novi prilozi za geologiju i metalogeniju rudnika gvožđa Ljubija.– Rudarski institute, Prijedor, 63–137.

HRVATOVIĆ, H. (2006): Geological guidebook through Bosnia and Herzegovina.– Geological Survey of Federation Bosnia and Herzegovina, Sarajevo, 163 p.

JEREMIĆ, M. (1958): Baritno-fluoritno ležište Žune kod Ljubije.– Rudarko-metalurški zbornik, 4, 465–474.

JURIĆ, M. (1971): Geologija područja sanskog paleozoika u sjeverozapadnoj Bosni.– Poseb. Izd. Geol. Glas., 11, 1–146.

LOKE, M.H., ACWORTH, I. & DAHLIN, T. (2003): A comparison of smooth and blocky inversion methods in 2D electrical imaging surveys.– Explor. Geophys., 34/3, 182–187. doi: 10.1071/EG03182

LOKE, M.H. & BARKER, R.D. (1996): Rapid least-squares inversion of apparent resistivity pseudosections by a quasi-Newton method.– Geophys. Prospect., 44, 131–152. doi: 10.1111/j.1365-2478.1996.tb00142.x

MEJU, M.A. (2002): Geoelectromagnetic Exploration for Natural Resources: Models, Case Studies and Challenges.– Surveys in Geophysics, 23, 133–205. doi: 10.1023/A:1015052419222

MILOŠEVIĆ, A., ALEKSEEV, A., ZAYTSEVA, E., NOVAK, M., KOLAR - JURKOVŠEK, T. & JURKOVŠEK, B. (2021): Late Carboniferous biota from the Ljubija iron mine area, Bosnia and Herzegovina.– Geologija, 64/(1), 65– 80, doi: 10.5474/geologija.2021.004

PALINKAŠ, A.L., BOROJEVIĆ ŠOŠTARIĆ, S., STRMIĆ PALINKAŠ, S., PROCHASKA, W., PÉCSKAY, Z., NEUBAUER, F. & SPANGENBERG, J.E. (2016): The Ljubija geothermal field: A herald of the Pangea break-up (NW Bosnia and Herzegovina).– Geol. Croat., 69/1, 3–30. doi: 10.4154/gc.2016.02

PAMIĆ, J. (1993): Eoalpine to Neoalpine magmatic and metamorphic processes in the northwestern Vardar Zone, the easternmost Periadriatic Zone and the southwestern Pannonian Basin.– Tectonophysics, 226/1–4, 503–518. doi: 10.1016/0040-1951(93)90135-7

PAMIĆ, J., GUŠIĆ, I. & JELASKA, V. (1998): Geodynamic evolution of the central Dinarides.– Tectonophysics, 297/1–4, 251–268. doi: 10.1016/S0040-1951(98)00171-1

SCHMID, S.M., BERZA, T., DIACONESCU, V., FROITZHEIM, N. & FÜGENSCHUH, B. (1998): Orogen-parallel extension in the Southern Carpathians.– Tectonophysics, 297/(1), 209–228. doi: 10.1016/S0040-1951(98)00169-3

SCHÖN, J.H. (2011): Physical Properties of Rocks - A Workbook.– In: CUBITT, J. (ed.): Vol. 8: Handbook of Petroleum Exploration and Production. Elsevier, Netherlands, 273–335.

STRMIĆ PALINKAŠ, S., SPANGENBERG, J.E. & PALINKAŠ A.L. (2009): Organic and Inorganic Geochemistry of Ljubija Siderite Deposits, NW Bosnia and Herzegovina.– Miner Deposita, 44, 893–913. doi 10.1007/s00126-009-0249-z

TELFORD, W.M., GELDART, L.P., SHERIFF, R.E. (1990): Applied Geophysics, 2nd Edt.– Cambridge University Press.

TOMLJENOVIĆ, B. (2002): Strukturne značajke Medvednice i Samoborskog gorja [*Structural characteristics of the Mt. Medvednica and the Samoborsko gorje Mt.* – in Croatian].– PhD Thesis, Faculty of Mining, Geology and Petroleum engineering, University of Zagreb, 208 p.

WARD, S.H. (1990): Resistivity and Induced Polarization Methods.– Geotechnical and Environmental Geophysics, Volume I: Review and Tutorial, 147–190. doi: 10.1190/1.9781560802785.ch6

WILLINGSHOFER, E. (2000): Extension in collisional orogenic belts: the Late Cretaceous evolution of the Alps and Carpathians.– PhD Thesis, Vrije University, Amsterdam, 146 p.